

## Bistable reaction–diffusion on a network

This content has been downloaded from IOPscience. Please scroll down to see the full text.

2015 J. Phys. A: Math. Theor. 48 075102

(<http://iopscience.iop.org/1751-8121/48/7/075102>)

View [the table of contents for this issue](#), or go to the [journal homepage](#) for more

Download details:

IP Address: 132.248.51.32

This content was downloaded on 29/01/2015 at 18:46

Please note that [terms and conditions apply](#).

# Bistable reaction–diffusion on a network

J-G Caputo<sup>1</sup>, G Cruz-Pacheco<sup>2</sup> and P Panayotaros<sup>2</sup>

<sup>1</sup>Laboratoire de Mathématiques, INSA de Rouen, Av. de l'Université, F-76801 Saint-Etienne du Rouvray, France

<sup>2</sup>Depto. Matemáticas y Mecánica, IIMAS-UNAM, Apdo. Postal 20-726, 01000 México DF, Mexico

E-mail: [caputo@insa-rouen.fr](mailto:caputo@insa-rouen.fr)

Received 30 June 2014, revised 12 December 2014

Accepted for publication 23 December 2014

Published 28 January 2015



CrossMark

## Abstract

We study analytically and numerically a bistable reaction–diffusion equation on an arbitrary finite network. We prove that stable fixed points (multi-fronts) exist for any configuration as long as the diffusion is small. We also study fold bifurcations leading to depinning and give a simple depinning criterion. These results are confirmed by using continuation techniques from bifurcation theory and by solving the time dependent problem near the threshold. A qualitative comparison principle is proved and verified for time dependent solutions, and for some related models.

Keywords: propagation in networks, reaction–diffusion, pinning condition

(Some figures may appear in colour only in the online journal)

## 1. Introduction

Discrete reaction–diffusion equations arise in many different fields. For example they can describe the propagation of a nerve impulse in a neuron [1] or the motion of a dislocation [2]. The solutions of these equations are typically fronts connecting two regions of constant value, say 0 and 1. Front pinning and propagation has been studied by many authors for a one dimensional network for a bistable cubic reaction term. An important result obtained by Keener [3] is that when the Laplacian is weak, any arbitrary configuration of 0s and 1s leads to a stable static solution. The study was extended by Erneux and Nicolis [4] who explicitly calculated these fronts and gave a pinning criterion. For material science applications and in the presence of an external forcing, Carpio and Bonilla [5] gave pinning conditions and estimated the front speed. For a two dimensional regular lattice, front propagation was studied by Hoffman and Mallet-Paret [6].

The present article considers arbitrary but finite networks, where to our knowledge there are no works. We address specifically this problem and study analytically and numerically

static fronts and how they destabilize in an arbitrary finite network (graph). The reaction term we use is the bistable cubic nonlinearity and the diffusion term is the standard graph Laplacian of the network (see e.g. [7]). Throughout the article, we refer to this equation as the Zeldovich model. We introduce and motivate the bistable reaction–diffusion system by considering how an epidemic front propagates on a network. To describe how the front moves on the network, we extend the standard Kermack–McKendrick model (see e.g. [8] for a recent application) to a network and show how it reduces to a discrete Fisher equation. In contrast to the one node model, the network Kermack–McKendrick model is not commonly used to describe the spread of an epidemic. The Fisher model only describes the propagation phase. The related Zeldovich model we propose is also new but its cubic bistable nonlinearity has a local excitation threshold, which may be a desirable feature for both geographic networks, where the epidemic spreads from one location to another, and agent-based networks, where the disease spreads from one individual to another.

A first result is the existence of static stable fronts for small diffusivity. The argument combines the implicit function theorem (as in the anticontinuous limit used for other lattice problems, see [9]) with small diffusivity asymptotics for the front amplitudes. The proof also uses a suitable definition for the interface between the active and quiescent sites. The statement is analogous to Keener’s result for the integer lattice [3]. We also show that for large diffusivity the only static solutions are spatially homogeneous.

The existence of these fronts depends on the diffusivity, the nonlinearity, and the local excitation threshold parameters of the model. We focus on the dependence of the static fronts on the diffusivity using numerical continuation techniques. The continuation exhibits the fold structure seen in one dimensional studies [4]. For general networks the depinning diffusivity threshold depends on the front configuration, and a static configuration that becomes unstable can be pinned elsewhere. We compute numerically the depinning thresholds for different static solutions and show that they can be predicted accurately by a simple heuristic expression derived for small diffusivity. By solving the time dependent problem, we verify these findings and see how the connectivity of the network affects the propagation of the fronts above the threshold.

We also obtain qualitative comparison results between different solutions of the Zeldovich equation, showing in particular that ‘large’ fronts involving large regions of 1s dominate ‘small’ fronts. Our study also contains comparison results showing that the Fisher equation describes faster front propagation than both the Zeldovich and Kermack–McKendrick equations. These results are also verified numerically. We see also that the Fisher and Kermack–McKendrick fronts propagate at comparable speeds and are much faster than the Zeldovich fronts. Finally we present numerical results for larger local excitation threshold parameters, showing that the static fronts become wider and travel much faster across the network when they destabilize.

The article is organized as follows. In section 2 we introduce the Zeldovich (bistable) equation and discuss the other models. Section 3 studies the fixed points of the Zeldovich equation, presenting theoretical and numerical continuation results, as well as a depinning criterion. Section 4 describes comparison results between the Zeldovich solutions and between the Zeldovich, Fisher, and Kermack–McKendrick solutions. Section 5 presents numerical results of the evolution problem; there we validate the pinning threshold for different fronts and compare the dynamics of large and small fronts. We also show that fronts become wider as the nonlinearity threshold increases and we compute the pinning threshold. Conclusions are given in section 6. Longer proofs of statements in sections 4 and 5 are in appendices A and B respectively.

## 2. Reaction–diffusion models on a network

Here we introduce the different models of reaction–diffusion on a network that we will consider. We use as an application the propagation of an epidemic. One of the main models to describe the time evolution of the outbreak of an epidemic is the Kermack–McKendrick model [10]

$$S_t = -\alpha SI, \quad (1)$$

$$I_t = \alpha SI - \beta I, \quad (2)$$

$$R_t = \beta I, \quad (3)$$

where  $S$ ,  $I$ ,  $R$  are respectively the number of people susceptible to be infected, the number of infected and the number of recovered in a total constant population  $N$  and where the  $t$  subscript represents the time derivative. We have of course  $S + I + R = N$ . The dynamics of the model is that  $I_t > 0$  (respectively  $I_t < 0$ ) if  $S > \beta/\alpha$  (respectively  $S < \beta/\alpha$ ). Roughly speaking, assuming that  $I(0)$  is near zero, and  $S(0) > \beta/\alpha$ , the infected population  $I(t)$  increases, reaches a maximum value and decreases to zero. The main questions are, what is the maximum value of  $I$ , what is the time to reach it, how large is the integral of  $I$  etc.

First, we rescale the variables by  $N$ ,  $s = S/N$ ,  $i = I/N$ ,  $r = R/N$ . This yields the system

$$s_t = -\alpha Nsi, \quad (4)$$

$$i_t = \alpha Nsi - \beta i, \quad (5)$$

$$r_t = \beta i. \quad (6)$$

Following Murray [11] we introduce now the possibility of spatial dispersion with a Laplacian term. The system for  $s$  and  $i$  can be written as

$$\begin{aligned} s_t &= \epsilon \Delta s - \gamma si, \\ i_t &= \epsilon \Delta i + \gamma si - \beta i, \end{aligned} \quad (7)$$

where  $\gamma = \alpha N$ . This model will describe the outbreak of the epidemic, its spreading, and eventual demise as  $i$  peaks and starts decreasing.

To concentrate on the dynamics leading to the maximum of the outbreak, we eliminate the  $\beta$  term. Then, to study the dynamics of a front, we can assume  $s + i = 1$  so that we get the Fisher equation

$$i_t = \epsilon \Delta i + \gamma(1 - i)i. \quad (8)$$

This equation has two homogeneous solutions  $i^* = 0, 1$  and the former is unstable. The model does not have a threshold as opposed to the Kermack–McKendrick. To re-introduce this important feature, we modify the nonlinearity into the cubic (Zeldovich) so that we get

$$u_t = \epsilon \Delta u + \gamma(1 - u)u(u - a). \quad (9)$$

For this, there are only two stable homogeneous solutions  $u^* = 0, 1$ . As discussed in the introduction, this equation has many physical applications; it is then an important physical model.

Up to this level, we considered three different models in a continuum space. Now we assume that the propagation occurs on a network. For this, as in [12], we replace the usual continuum Laplacian  $\Delta$  by the graph Laplacian. As an example, consider the propagation of an epidemic from city to city, in the network of the six major cities of Mexico, shown in figure 1. The model is then

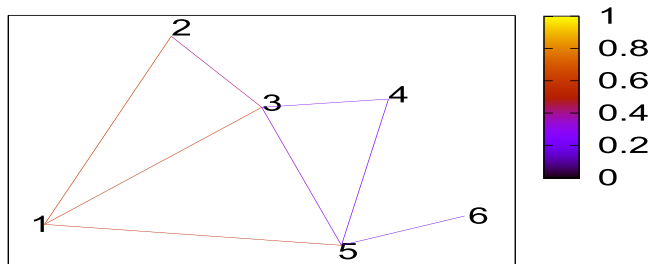


**Figure 1.** Graph of the six main cities in Mexico numbered from 1 to 6: Guadalajara, Zacatecas, Queretaro, Pachuca, Mexico City, Puebla. The links represent the main roads connecting these cities. The colors represent a front starting from node 1, propagating across the network.

$$u_t = \epsilon \Delta u + \gamma(1 - u)u(u - a), \tag{10}$$

where  $u = (u_1, u_2, \dots, u_6)^T$  is the vector representing the nodes (cities). The links correspond to the main roads connecting these cities.

For this particular example, the graph Laplacian  $\Delta$  is

$$\Delta \equiv \begin{pmatrix} -3 & 1 & 1 & 0 & 1 & 0 \\ 1 & -2 & 1 & 0 & 0 & 0 \\ 1 & 1 & -4 & 1 & 1 & 0 \\ 0 & 0 & 1 & -2 & 1 & 0 \\ 1 & 0 & 1 & 1 & -4 & 1 \\ 0 & 0 & 0 & 0 & 1 & -1 \end{pmatrix}. \tag{11}$$

In the following, we study the three different models, the Zeldovich (9), Fisher (8) and Kermack–McKendrick (7) on a network.

Note that the graph Laplacian  $\Delta$  is a non-negative symmetric matrix [7]. We use this property below. In physical units the parameter  $\epsilon$  is

$$\epsilon = \frac{D}{h^2}, \tag{12}$$

where  $D$  is a diffusion coefficient and  $h$  is a typical distance between cities. The typical time for the diffusion is then

$$t = \frac{1}{\epsilon} = \frac{h^2}{D}. \tag{13}$$

At this time we assumed the same diffusion coefficient (weight) for all the links of the network. If a node is closer or farther from its neighbors one could modify the coefficients in  $\Delta$ . With this generalization, we would still have a positive symmetric graph Laplacian.

Let  $\tau$  be the triangle  $\{(s, i) \in [0,1]^2, s + i \leq 1\}$ . We have the following result.

**Lemma 2.1.** *The unit cube  $[0,1]^N$  is invariant under the evolution of the Zeldovich (9) and Fisher (8) equations in  $\mathbf{R}^N$ . The product of the triangles  $\tau^N$  is invariant under the Kermack–McKendrick (7) system with in  $\mathbf{R}^{2N}$ .*

This means that the models are consistent, the solutions remain physical ( $\geq 0$  and  $\leq 1$ ). The lemma follows from propositions 4.1 and 4.4 in section 4 below (these do not use any of

the results of section 3). It is also easy to show that the corresponding vector fields point inwards at the boundaries.

### 3. Fixed points of the Zeldovich model

We want to describe a situation where only some nodes are excited; in the epidemic context, it means that some nodes are infected and the rest are susceptible. Only the Zeldovich model (9) has such stable fixed points; these are generalized static ‘fronts’ where some nodes are close to one and the rest close to zero. Therefore, in this section, we concentrate on the fixed points of the Zeldovich model (9). We will clarify the situation for the Fisher model (8) below and show why it is less interesting. For definiteness, throughout this section, we consider the six node graph from figure 1; it is clear that the results can be extended to an arbitrary finite graph.

In the following, and throughout the article we use  $x$  to denote the field. The fixed point equation we solve is

$$F(x, \epsilon) = 0, \quad x = [x_1, \dots, x_n]^T, \quad (14)$$

where

$$F_k(x, \epsilon) = \epsilon(\Delta x)_k + f_k(x), \quad \text{with} \quad (15)$$

$$f_k(x) = \gamma(1 - x_k)x_k(x_k - a), \quad k = 1, \dots, n, \quad (16)$$

$\Delta$  is the graph Laplacian of (11), and  $0 < a < 1, \gamma = 1$ . We will examine how the fixed points depend on the coupling parameter  $\epsilon \geq 0$ .

For  $\epsilon = 0$ , and every partition of the set of nodes into three subsets  $S_0, S_a, S_1$  we have a solution of  $F(x, 0) = 0$  of the form  $x_j = 0$ , if  $j \in S_0, x_j = a$ , if  $j \in S_a, x_j = 1$ , if  $j \in S_1$ . Clearly, these are the only solutions of  $F(x, 0) = 0$ . An inspection of the Jacobian reveals that when  $S_a$  is empty, these solutions are stable. On the other hand if  $S_a$  is nonempty these solutions are unstable. The number of unstable direction is the number of sites in  $S_a$ . The solutions where  $S_a$  is empty are generalizations of the fronts that exist for the one dimensional case, they are the main subject of interest of the article.

#### 3.1. Homogeneous fixed points

Let us now consider the case  $\epsilon > 0$ . The homogeneous fixed points can be analyzed for arbitrary  $\epsilon$ . For that consider the system linearized around the fixed point  $x^*$

$$v_i = \left[ \epsilon\Delta + Df(x^*) \right] v, \quad (17)$$

where the Jacobian matrix has elements

$$Df(x^*) = \delta_{k,m} \gamma \left( 2(1 + a)x_k^* - 3x_k^{*2} - a \right). \quad (18)$$

When the fixed points are homogeneous,  $DN$  has a very simple form, it can be written

$$Df = -\gamma a I, \quad Df = \gamma(a - 1)I, \quad Df = \gamma a(1 - a)I$$

respectively for  $x^* = [0, \dots, 0]^T, x^* = [1, \dots, 1]^T, x^* = [a, \dots, a]^T$ , where  $I$  is the  $N \times N$  identity. The matrix  $Df$  is then  $cI$  for some real constant  $c$ , and  $\sigma(\epsilon\Delta + Df(x^*))$  is  $\sigma(\epsilon\Delta) + c$ . To study the stability it is then convenient to use the basis of orthogonal eigenvectors of the symmetric matrix  $\Delta$  [7]

$$\Delta V^k = -\omega_k^2 V^k,$$

where the eigenfrequencies  $\omega_k$  verify

$$\omega_1 = 0 \leq \omega_2 \leq \dots \leq \omega_n.$$

We write

$$i = \alpha_1 V^1 + \alpha_2 V^2 \dots + \alpha_n V^n. \tag{19}$$

Plugging the above expression into (18) we get the evolution of the amplitude

$$\dot{\alpha}_k = -[\epsilon \omega_k^2 + a] \alpha_k \tag{20}$$

for the fixed point  $x^* = [0, \dots, 0]^T$ . Clearly it is stable for any  $\epsilon$ . In a similar way we can show that  $x^* = [1, \dots, 1]^T$  is always stable. The fixed point  $x^* = [a, \dots, a]^T$  is always unstable since we have an eigenvalue  $-\epsilon \omega_1^2 + \gamma a(1 - a) > 0$ .

### 3.2. Non homogeneous fixed points

For the non-homogeneous fixed points the analysis is not so simple. Let us first consider the case  $\epsilon > 0$  but small. The implicit value theorem implies that each solution  $x_0$  of  $F(x, 0) = 0$  can be continued uniquely, that is, it belongs to a unique smooth one-parameter family of  $x(\epsilon)$  satisfying  $F(x(\epsilon), \epsilon) = 0, x(0) = x_0$ , provided that  $|\epsilon|$  is sufficiently small, see e.g. [13]. The solution  $x(\epsilon)$  of the local branch passing from  $x(0)$  has the same stability as  $x(0)$ , for  $|\epsilon|$  sufficiently small. This follows from the fact that all the solutions  $x(0)$  are hyperbolic.

The numerical solutions below were obtained using the minpack implementation of Powell's hybrid Newton method [14]. We start from  $\epsilon = 0$ , solving (14) using Newton's method and step in  $\epsilon$ . After some  $\epsilon$ , we continue stepping but use the pseudo-arc as a parameter [15] because we anticipate a fold. The linear stability of a solution  $x(\epsilon_0)$  is computed readily by examining the eigenvalues of  $D_1 F(x, \epsilon)$  at  $x(\epsilon_0), \epsilon_0$ , i.e.

$$(D_1 F(x, \epsilon))_{n,m} = \epsilon \Delta_{n,m} + \delta_{n,m} \gamma (2(1 + a)x_n - 3x_n^2 - a). \tag{21}$$

We see numerically that all solutions of  $F(x, \epsilon) = 0$  with  $\epsilon > 0$  satisfy  $x_j \in (0, 1)$ , for all  $j \in \{1, \dots, 6\}$ . This is also shown in corollary 3.4 below. As we increase the value of  $\epsilon$  along a branch of solutions continued from an  $\epsilon = 0$  solution  $x_0$ , the linear stability remains unchanged, until some  $\epsilon_0$ , depending on the branch, where we see a fold. The branch is then continued by decreasing  $\epsilon$ , until we reach a different solution  $\tilde{x}(0)$  of the  $\epsilon = 0$  problem. After the fold the number of stable and stable eigenvalues changes. We observe that when  $x(0)$  is stable, the branch changes stability at the fold, and  $\tilde{x}(0)$  is unstable. For example, setting  $a = 0.1$ , we see that the unstable  $\epsilon = 0$  solution  $[1, 1, 1, 0, 0.1, 0]^T$  is connected to the stable  $\epsilon = 0$  solution  $[1, 1, 1, 0, 0, 0]^T$  by a branch that has a fold at  $\epsilon = 0.001\ 310\ 357\ 64$ . In figure 2 we show the value of the component  $x_5$  at different values of  $\epsilon$  of the fixed point. The other components start, and finish at the same values.

A similar behavior was observed for all the examples examined, except the spatially homogeneous solutions  $c[1, \dots, 1]^T$  with  $c = 1, a$ , or  $0$ . From relation (16) one can see that these exist for all  $\epsilon$ . Based on our numerical observations we conjecture that all  $3^6 - 3$  inhomogeneous fixed points of the  $\epsilon = 0$  problem (we exclude the spatially homogeneous solutions) belong to branches undergoing a fold bifurcation at some positive value of  $\epsilon$ , i.e. we have  $(3^6 - 3)/2$  branches with folds, connecting pairs of  $\epsilon = 0$  solutions. This conjecture can be checked numerically by continuing all  $\epsilon = 0$  fixed points. From the theoretical point of

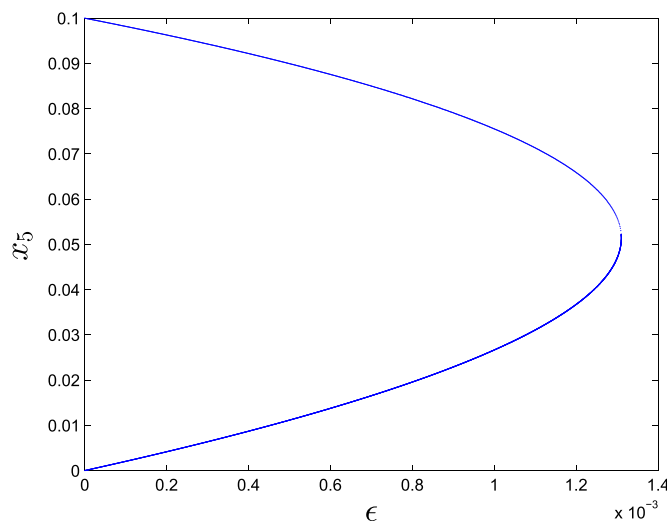


**Figure 2.** Component  $x_5$  versus  $\epsilon$  for a branch connecting the  $\epsilon = 0$  fixed points  $[1, 1, 1, 0, 0, 0, 0, 0]^T$  and  $[1, 1, 1, 0, 0, 0, 0, 0]^T$ .

view we can also show that non-spatially homogeneous fixed points cannot exist for arbitrarily large  $\epsilon$ . We have

**Proposition 3.1.** *There is an  $\epsilon_c > 0$ , such that all  $(x, \epsilon)$ ,  $x \in I^N$ ,  $\epsilon > \epsilon_c$  that satisfy  $F(x, \epsilon) = 0$  are of the form  $x = c[1, \dots, 1]^T$ , with  $c = 0, a$ , or  $1$ .*

The proof is given in appendix A. The dynamical importance of  $\epsilon_c$  will be discussed further in the next section. The general idea is that for  $\epsilon > \epsilon_c$  all initial conditions ( $\neq a[1, \dots, 1]^T$ ) should go to one of the two fixed points  $c[1, \dots, 1]^T$ ,  $c = 1, 0$ , as  $t \rightarrow \infty$ .

An interesting problem is the computation of  $\epsilon_c$ . One idea is to continue all branches starting at  $\epsilon = 0$  solutions and find the largest value  $\epsilon_0$  of a fold. This computation would give a lower estimate of  $\epsilon_c$ , since we can not at present rule out the possibility of fixed points not belonging to these branches. Also it is of interest to see whether we can have a family of fixed points  $x(\epsilon)$  that are stable for  $\epsilon$  arbitrarily close to  $\epsilon_c$ , e.g. a continuous branch having a fold with change of stability at  $\epsilon_c$ . To obtain a first estimation of  $\epsilon_c$  we have examined numerically all branches starting from stable  $\epsilon = 0$  solutions for a fixed value of  $a$ . There are  $2^6 - 2$  such branches (we exclude  $c[1, \dots, 1]^T$ , with  $c = 1, 0$ ). These are solutions  $x(0)$  with  $S_a = \emptyset$ . In all (non-spatially homogeneous) cases these solutions are connected to an unstable solution  $\tilde{x}(0)$  of the  $\epsilon = 0$  problem, with  $S_a \neq \emptyset$ . For  $a = 0.1$ , the largest value of the fold coupling  $\epsilon_0$  is  $\bar{\epsilon}_0 = 0.002\,998\,352\,24$ , and is observed for the branch connecting the  $\epsilon = 0$  solutions  $[0, 0, 0, 0, 0, 1]^T$  and  $[0, 0, 0, 0, 0.1, 1]^T$ .

Note that the  $\epsilon = 0$  solution  $[0, 0, 0, 0, 0, 1]^T$  has only one neighbor. This is read from the Laplacian (11). It is reasonable to expect that the solutions that are the last to exist have the least neighbors. We see from (11) that all other  $\epsilon = 0$  solutions with  $|S_1| = 0$  have more than two neighbors, and it is observed that the corresponding branches undergo folds at smaller values of  $\epsilon$ . For example the branch starting from  $[0, 0, 0, 1, 0, 0]^T$ , with two neighbors by (11), undergoes a fold at  $\epsilon_0 = 0.002\,813\,136\,77$ , while the branch starting from  $[0, 0, 0, 0, 1, 0]^T$ , with four neighbors, undergoes a fold at  $\epsilon_0 = 0.002\,529\,277\,87$ . The

**Table 1.** Critical  $\epsilon$  for the ‘generalized front’ to destabilize for different initial conditions.

Connectivity	Node	Branch	$\epsilon_0$	$\epsilon_0$	Expression (23)
			From time evolution	Continuation	
1	6	$[0, 0, 0, 0, 0, 1]^T$	$3.0 \times 10^{-3}$	$2.998 \times 10^{-3}$	$2.97 \times 10^{-3}$
2	2	$[0, 1, 0, 0, 0, 0]^T$	$2.7 \times 10^{-3}$	$2.547 \times 10^{-3}$	$2.79 \times 10^{-3}$
4	3	$[0, 0, 1, 0, 0, 0]^T$	$2.54 \times 10^{-3}$	$2.528 \times 10^{-3}$	$2.63 \times 10^{-3}$
2	1 2 3	$[1, 1, 1, 0, 0, 0]^T$	$1.31 \times 10^{-3}$	$1.310 \times 10^{-3}$	$1.32 \times 10^{-3}$

notion of neighbors can be extended to ( $|S_a| = 0$ )  $\epsilon = 0$  solutions with  $|S_1| > 1$ . In such cases we can look for the number of external connections to the set  $S_1$ , i.e. the number of points having distance one from  $S_1$ . We see that more sites in  $S_1$  generally imply lower  $\epsilon_0$  in the corresponding branch. For example the branch starting from  $[1, 1, 1, 1, 1, 0]^T$ , where  $S_1$  has one external connection, undergoes a fold at  $\epsilon_0 = 0.002\,506\,944\,32$ . This is lower than the value of the fold value  $\epsilon_0$  of the branch starting from  $[0, 0, 0, 1, 0, 0]^T$  above, with two neighbors but fewer peaks. Comparing the values of  $\epsilon_0$  for the branches corresponding to  $[0, 0, 0, 0, 0, 1]^T$  and  $[1, 1, 1, 1, 1, 0]^T$ , we also see that complementary  $\epsilon = 0$  solutions  $x(0)$ ,  $x'(0)$  (with  $|S_a| = 0$ ), i.e. ones with  $S_1(x(0))$ ,  $S_1(x'(0))$  that are disjoint and whose union is the set of all nodes, generally have corresponding branches with different fold values.

The  $\epsilon = 0$  solutions not considered in the above enumeration are expected to correspond to branches of solutions that are linearly unstable. Thus, even if we find a static solution such that  $\epsilon_0 > \bar{\epsilon}_0 = 0.002\,998\,352\,24$ , we expect that for  $\epsilon > \bar{\epsilon}_0$ , almost all initial conditions of the time dependent system (9) go to either  $c[1, \dots, 1]^T$ ,  $c = 1, 0$ , as  $t \rightarrow \infty$ .

### 3.3. The pinning criterion

In this section we establish a pinning criterion using the asymptotics from the previous section. To better understand how  $\epsilon_0$  depends on the type of front and node connectivity, we develop a simple argument that assumes  $\epsilon_0$  is small, and that all sites except one that we call  $n_c$  have values  $1 + O(\epsilon)$ , or  $O(\epsilon)$ , see section 3.3 below. This is consistent with what we see numerically, namely that the node that is destabilized first has value approximately  $a/2$ , see e.g. figure 2. Other sites have values that are much lower. The argument is as follows. Call  $x$  the value of the node  $n_c$  that will first destabilize. Then the equation at  $n_c$  for  $x$  is

$$\epsilon(N - Kx + O(\epsilon)) + x(1 - x)(x - a) = 0,$$

where  $N$  is the number of neighbors of  $n_c$  that are at 1 and  $K$  is the connectivity of  $n_c$ . This yields

$$\epsilon = \frac{x(1 - x)(x - a)}{Kx - N}. \tag{22}$$

From the continuation study of the static solutions we have seen that for

$$\epsilon = \epsilon_0, \quad x \approx a/2.$$

Combining this observation with (22) yields the estimate for

$$\epsilon_0 = \frac{a^2}{4} \frac{2 - a}{2N - Ka}. \tag{23}$$

This means that for  $\epsilon < \epsilon_0$  the specific front is stationary while it travels for  $\epsilon > \epsilon_0$ . This estimate is reported in table 1, together with the  $\epsilon_0$  found numerically. For  $a$  relatively small, e.g. for  $a = 0.1$  used here, we see excellent agreement.

### 3.4. Asymptotics of the fixed points

In what follows we show some general results on the profile of the fixed points of (9) for  $\epsilon > 0$ , and small. We estimate the decay of the fixed point profiles away from the sites where the solution is near unity; we also see that we can obtain small  $\epsilon$  asymptotics for  $x(\epsilon)$  at all sites. For instance, we show that the amplitude  $x_n(\epsilon)$  of the equilibrium at the site  $n$  is

$$x_n(\epsilon) = 1 + O(\epsilon^{d_n}),$$

where  $d_n$  is the distance of site  $n$  from the analogue of the ‘interface’ of the  $\epsilon = 0$  configuration, see lemma A.1. Roughly speaking, the interface or ‘front’ of an  $\epsilon = 0$  configuration, defined more precisely below, consists of the sites where the solution jumps from zero to unity. The small  $\epsilon$  asymptotic gives us information on the decay of the  $x_n(\epsilon)$  as we move away from the sites that are near unity. For sites with value near unity it also tells us that are further away from the interface have values that are much closer to unity.

Proposition 3.3 can be also used to compare small  $\epsilon$  solutions continued from different  $x(0)$ , see corollary 3.6 below.

The proof of proposition 3.3 is based on small- $\epsilon$  expansions

$$x_n(\epsilon) = \sum_{m=0}^{\infty} a_{n,m} \epsilon^m,$$

valid for all sites  $n$ . The idea is to insert these expression into (16) and examine the coefficients of the series. We first obtain a less precise, intermediate statement, lemma A.1, using induction on the distance from the ‘interface’ between ones and zeros of the  $\epsilon = 0$  solutions. proposition 3.3 uses the same strategy, and lemma A.1.

The precise statements use the following definitions and notation. Let  $\text{nbr}(n)$  denote the sites adjacent to the site  $n$ . Let  $c_n = |\text{nbr}(n)|$ . Let  $\text{dist}(R, n)$  denote the distance between the set of sites  $R$ , and a node  $n$ .

**Definition 3.2.** Given a nontrivial solution  $x(0)$  of the  $\epsilon = 0$  equation  $F = 0$ , denote by  $S_1, S_a, S_0$  the sets of indices  $n$  where  $x_n = 1, a, 0$  respectively. Also let  $S_A = S_1 \cup S_a$ . The interface  $I$  of the front is the set of nodes  $n \in S_1$  having at least one neighbor  $j \in S_a \cup S_0$ .

Then we have:

**Proposition 3.3.** Let  $x(0)$  be a nontrivial solution of equations (14), (16) with  $\epsilon = 0$ , and let  $x(\epsilon), \epsilon \in [0, \epsilon_0]$  denote the unique branch of solutions of  $F = 0, \epsilon > 0$ , that continue  $x(0)$  for  $\epsilon \geq 0$ . Consider the sets  $S_1, S_a, S_0$ , and  $I$  corresponding to  $x(0)$  as defined above, with  $S_b, I$  nonempty. Then for  $\epsilon > 0$  sufficiently small we have that (i)  $n \in S_0, \text{dist}(S_A, n) = m \geq 1$  imply

$$x_n(\epsilon) = a_{n,m} \epsilon^m + O(\epsilon^{m+1}), \quad \text{with } a_{n,m} > 0, \tag{24}$$

and (ii)  $n \in S_1$ ,  $\text{dist}(I, n) = m \geq 0$  imply

$$x_n(\epsilon) = 1 + a_{n,m+1}\epsilon^{m+1} + O(\epsilon^{m+2}), \quad \text{with } a_{n,m+1} < 0, \quad (25)$$

The proof is given in appendix A. An immediate consequence is:

**Corollary 3.4.** *Let  $x(0)$  be a nontrivial solution equation (16) with  $\epsilon = 0$ , and let  $x(\epsilon)$ ,  $\epsilon \in [0, \epsilon_0]$  denote the unique branch of solutions of (16),  $\epsilon > 0$ , that continue  $x(0)$  for  $\epsilon \geq 0$ . Then for  $\epsilon > 0$  and sufficiently small we have  $x_n(\epsilon) \in (0, 1)$ , for all sites  $n$ .*

**Proof.** For sites  $n \in S_a$  we have  $x_n(\epsilon) = a + O(\epsilon) \in (0, 1)$  for  $\epsilon$  sufficiently small. For other sites the statement follows from proposition 3.3.  $\square$

**Remark 3.5.** The above asymptotic appears to be related to the estimate of  $\epsilon_0$  in (23), and the assumption that the all sites  $n \neq n_c$  have values  $1 + O(\epsilon)$ , and  $O(\epsilon)$ . Indeed most sites  $n \neq n_c$  are seen to be  $O(\epsilon)$  from their  $\epsilon = 0$  values at  $\epsilon_0$ . Note however that the site  $n_c$  also has the value 0 (or  $\alpha$ ) at  $\epsilon = 0$ , and comes near  $a/2$  as  $\epsilon$  approaches  $\epsilon_0$ . The use of the small- $\epsilon$  asymptotic in justifying (23) is then not clear.

Another consequence of proposition 3.3 is that for  $\epsilon > 0$  sufficiently small there exist pairs of static solutions  $x, y$  of the Zeldovich equation satisfying  $x_n < y_n, \forall n \in \{1, \dots, N\}$ . The construction is as follows:

**Corollary 3.6.** *Let  $x(\epsilon), y(\epsilon)$ ,  $\epsilon$  sufficiently small, be continuations of the  $\epsilon = 0$  fixed points  $x = x(0), y = y(0)$  of the Zeldovich equation satisfying*

$$(i) \quad S_\alpha(x) = S_\alpha(y) = \emptyset, \quad (ii) \quad S_1(x) \subset S_1(y), \quad (26)$$

$$(iii) \quad \text{dist}(I(x), n) < \text{dist}(I(y), n), \quad \forall n \in S_1(x) \cup S_1(y), \quad (27)$$

$$(iv) \quad \text{dist}(S_1(x), n) > \text{dist}(S_1(y), n), \quad \forall n \in S_0(x) \cup S_0(y). \quad (28)$$

Then for all  $\epsilon > 0$  sufficiently small we have  $x_n(\epsilon) < y_n(\epsilon), \forall n \in \{1, \dots, N\}$ .

This means that the order that exists between fronts for  $\epsilon = 0$  will remain for  $\epsilon > 0$ .

**Proof.** We consider the three cases  $n \in S_0(x) \cup S_1(y)$ ,  $S_1(x) \cup S_1(y)$ , and  $S_0(x) \cup S_0(y)$ . By (ii)  $S_1(x) \cup S_0(y) = \emptyset$ . For  $n \in S_0(x) \cup S_1(y)$  we have

$$y_n(\epsilon) = 1 - O(\epsilon) > x_n(\epsilon) = O(\epsilon),$$

for  $\epsilon > 0$  small.

For  $n \in S_1(x) \cup S_1(y)$ , proposition 3.3 yields

$$x_n(\epsilon) = 1 - |a_{n,m+1}| \epsilon^{m+1} + O(\epsilon^{m+2}),$$

$$y_n(\epsilon) = 1 - |a_{n,\tilde{m}+1}| \epsilon^{\tilde{m}+2} + O(\epsilon^{\tilde{m}+2}),$$

with  $a_{n,m}, a_{n,\tilde{m}+1} \neq 0$ , and

$$m = \text{dist}(I(x), n), \quad \tilde{m} = \text{dist}(I(y), n), \quad \tilde{m} > m.$$

Therefore  $y_n(\epsilon) > x_n(\epsilon)$  for  $\epsilon > 0$  small enough.

For  $n \in S_0(x) \cup S_0(y)$ , proposition 3.3 yields

$$\begin{aligned} x_n(\epsilon) &= |a_{n,\mu}| \epsilon^\mu + O(\epsilon^{\mu+1}), \\ y_n(\epsilon) &= |a_{n,\tilde{\mu}}| \epsilon^{\tilde{\mu}} + O(\epsilon^{\tilde{\mu}+1}), \end{aligned}$$

with  $a_{n,\mu}, a_{n,\tilde{\mu}+1} \neq 0$ , and

$$\mu = \text{dist}(I(x), n), \quad \tilde{\mu} = \text{dist}(I(y), n), \quad \mu > \tilde{\mu}.$$

Again  $y_n(\epsilon) > x_n(\epsilon)$  for  $\epsilon > 0$  small enough. □

#### 4. Ordering of different front solutions

In this section, we will compare the time dependent solutions of the Zeldovich equation, the Fisher and the Kermack–McKendrick models. We first consider the time dependent solutions of the Zeldovich equation (9), and establish qualitative comparison (or monotonicity) results for different solutions of the Zeldovich model, see proposition 4.1. An application is corollary 4.2, a stability statement for some of the static solutions discussed in corollary 3.6 of the previous section. Another goal is to compare the Zeldovich model with the original Kermack–McKendrick system, and the intermediate Fisher system. We show that the Fisher model describes a faster propagation of the front than both the Zeldovich and Kermack–McKendrick models, see propositions 4.3, 4.4 respectively. In the next section we show some numerical examples.

The comparison statements below use a notion of ‘partial order’ between configurations. In particular  $u < n$  (respectively  $u \leq v$ ), with  $u, v \in [0,1]^N$ , will mean  $u_n < v_n$  (respectively  $u_n \leq v_n$ ),  $\forall n \in \{1, \dots, N\}$ . We also let  $\mathbf{0} = [0, \dots, 0]^T$ ,  $\mathbf{1} = [1, \dots, 1]^T \in [0,1]^N$ . A ‘larger’ configuration thus describes a state where the front is more advanced at all sites.

**Proposition 4.1.** *Let  $T > 0$ ,  $x, y: [0, T] \rightarrow [0,1]^N$  be two solutions of (either) the Zeldovich (9) (or the Fisher (8)) equation, with initial conditions satisfying  $\mathbf{0} < x(0) < y(0) \leq \mathbf{1}$ . Then  $x(t) < y(t)$ ,  $\forall t \in [0, T]$ .*

This means that the ‘larger’ fronts, ie the ones that involve more nodes, will always move ahead of the ‘smaller’ fronts.

Since both vectors  $\mathbf{0}$ ,  $\mathbf{1}$  are static solutions of the Zeldovich and Fisher equations, lemma 2.1 is a special case of proposition 4.1.

**Corollary 4.2.** *Let  $T > 0$ . Let  $x, y \in [0,1]^N$  be two static solutions of the Zeldovich equation satisfying  $x < y$ , and let  $u: [0, T] \rightarrow [0,1]^N$  be a solution of the Zeldovich equation with initial condition  $u(0)$  satisfying  $x < u(0) < y$ . Then  $x < u(t) < y$ ,  $\forall t \in [0, T]$ .*

This result states that the order of the fronts will remain during the propagation. This is connected to the existence of pairs of static solutions of the Zeldovich equation satisfying  $x < y$  (corollary 3.6). It allows to predict the dynamics of complicated fronts using the one of simpler ones.

We now compare solutions of the Fisher and Zeldovich equations.

**Proposition 4.3.** *Let  $T > 0$ . Let  $x_F, x_Z: [0, T] \rightarrow [0, 1]^N$  be solutions of the Fisher (8), and Zeldovich (9) equations respectively, with corresponding initial conditions satisfying  $\mathbf{0} < x_Z(0) \leq x_F(0) \leq \mathbf{1}$ . Then  $x_Z(t) \leq x_F(t), \forall t \in (0, T)$ .*

**Proposition 4.4.** *Let  $T > 0$ . Let  $x_F: [0, T] \rightarrow [0, 1]^N$  be a solution of the Fisher equation (8), and let  $(s, i): [0, T] \rightarrow \tau^N$  satisfy the Kermack–McKendrick system (7). Suppose also that the corresponding initial conditions satisfy  $i(0) < x_F(0)$ . Then  $i(t) \leq x_F(t), \forall t \in [0, T]$ .*

The above comparison statements follow from analogous statements for discrete time approximations of the solutions of the three equations. The approximations we use are obtained by the first-order explicit Euler method. We give proofs in appendix B.

## 5. Numerical results on front propagation

In the first part of this section we solve numerically the Zeldovich system (9) for initial conditions that are near the computed static solutions. We confirm the results of section 3 on thresholds, and examine the evolution of the front-like initial conditions for couplings that are above the threshold. In the second part we verify some of the predictions of the comparison results of section 4. One main observation is that the propagation of the Fisher, and Kermack–McKendrick models is much faster than the ones seen in the Zeldovich models. A third part examines the propagation of Zeldovich fronts for larger values of the local excitation threshold  $a$ . We can then observe very rapid front propagation. In all simulations below we use the variable step 5–6 dopri5 solver of Hairer *et al* [16] in double precision with a relative tolerance of  $10^{-10}$ .

### 5.1. Time evolution of the Zeldovich fronts

Branches of static solutions  $x(\epsilon)$  are labeled by the corresponding  $\epsilon \rightarrow 0$  limit  $x(0)$ , obtained by decreasing  $\epsilon$ . The value of  $\epsilon$  at the fold is  $\epsilon_0(x(0))$  (or simply  $\epsilon_0$  when the branch in question is clear). In addition to the numerical and theoretical  $\epsilon_0$  values from section 3, we here obtain a third estimate of  $\epsilon_0$  by integrating (9) starting with  $\epsilon < \epsilon_0$  and increasing  $\epsilon$  slowly on each run. The typical behavior is the following. For small  $\epsilon$  we always find a static solution. As  $\epsilon$  is increased past a threshold  $\epsilon_0$ , the solution destabilizes and gives rise to the homogeneous flat state  $[1, \dots, 1]^T$ . This estimated  $\epsilon_0$  is between the largest  $\epsilon$  leading to convergence to a similar static front, and the smallest  $\epsilon_0$  leading to a trajectory that diverges from the front. The three estimates of  $\epsilon_0$  are given in table 1 for some examples, and confirm the results expected from section 3.

We now present some examples of the evolution slightly above the  $\epsilon_0$  for different configurations. We examine how the connectivity of a node influences the destabilization of a front centered at that node.

In the first example we consider the evolution from an initial condition near a static front localized at node 6 which (with connectivity 1). The front belongs to the branch of  $[0, 0, 0, 0, 0, 1]^T$ , which is expected to be last to be destabilized. We use  $\epsilon = 3.0 \times 10^{-3}$ , slightly above the computed threshold  $\epsilon_0 = 2.998 \times 10^{-3}$ , and the initial condition

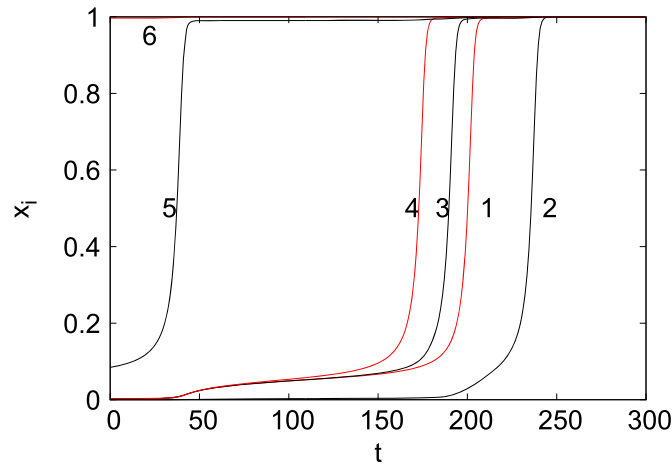


**Figure 3.** Time evolution of the different nodes for an initial front solution centered on node 6, of connectivity 1, with  $\epsilon = 3.0 \times 10^{-3}$  and the initial condition (29).

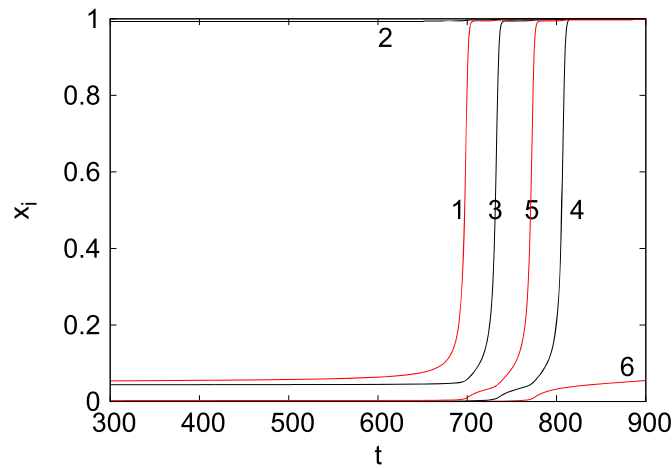


**Figure 4.** Time evolution of the different nodes for an initial front solution centered on node 2, of connectivity 2,  $\epsilon = 2.6875 \times 10^{-3}$  and the initial condition in (30).

$$\left[ 1.536 \times 10^{-3}, 8.680 \times 10^{-5}, 1.537 \times 10^{-3}, 1.578 \times 10^{-3}, 5.350 \times 10^{-2}, 0.997 \right]^T. \quad (29)$$

Notice how it decays very rapidly from the node 5 to the nodes 1 and 4 then node 3. The evolution is shown in figure 3, we see that the wave goes successively from 5, 4, 3, 1 and 2.

In the second example we consider an initial condition near the static solutions of the branch  $[0, 1, 0, 0, 0, 0]^T$ . We use  $\epsilon = 2.6875 \times 10^{-3}$ , which is slightly above computed  $\epsilon_0 = 2.547 \times 10^{-3}$  for the branch, and the initial condition

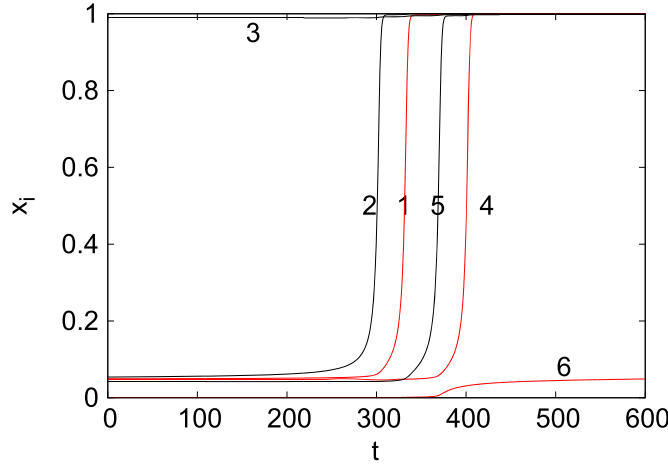


**Figure 5.** Time evolution of the different nodes for an initial front solution centered on node 3, of connectivity 4,  $\epsilon = 2.54 \times 10^{-3}$  and the initial condition in (31).

$$\left[ 5.088 \times 10^{-2}, 0.994, 4.298 \times 10^{-2}, 1.165 \times 10^{-3}, 2.35 \times 10^{-3}, 6.132 \times 10^{-5} \right]^T. \quad (30)$$

The value  $x_1 = 5.088 \times 10^{-2}$  is very close to  $a/2$  which is the value observed by the continuation method for  $\epsilon = \epsilon_c$ . The evolution is shown in figure 4. The solution destabilizes following the fixed point so  $x_1$  and  $x_3$  remain close to  $a/2$  for a long time before going to 1. We see that the wave follows the connectivity as it propagates from node 1 (3) to node 3 (4). Then node 5 (4) destabilizes and finally node 4. Node 6 is just destabilizing for  $t = 900$ . There are then different time scales in the dynamics depending on the connectivity.

We also note that  $\epsilon$  is greater than the threshold  $\epsilon_0 = 2.5 \times 10^{-3}$  for the branch  $[1, 1, 1, 1, 1, 0]^T$  (see section 3), this means that the front will not stop at node 5, it will also destabilize node 6.

We now consider an initial condition centered on node 3, near static solutions of the branch  $[0, 0, 1, 0, 0, 0]^T$ . We use  $\epsilon = 2.54 \times 10^{-3}$ , which is slightly above the computed threshold  $\epsilon_0 = 2.528 \times 10^{-3}$  for the branch, and the initial condition

$$\left[ 4.946 \times 10^{-2}, 5.404 \times 10^{-2}, 0.989, 4.785 \times 10^{-2}, 4.206 \times 10^{-2}, 1.054 \times 10^{-3} \right]^T. \quad (31)$$

The evolution given in figure 5 shows that the front centered on node 3 of connectivity 4 destabilizes in the same way as the one centered on node 2 except that now nodes 2, 1, 5 and 4 have values around  $a/2$  for a long time. Node 6 will destabilize after a long time. As in the previous example  $\epsilon$  is greater than the threshold  $\epsilon_0 = 2.5 \times 10^{-3}$  for the branch  $[1, 1, 1, 1, 1, 0]^T$ .

We now study initial conditions near static solutions of the branch  $[1, 1, 1, 0, 0, 0]^T$ , see figure 6. We use  $\epsilon = 1.32 \times 10^{-3}$ , slightly above the critical  $\epsilon_0 = 1.3103 \times 10^{-3}$  (see section 4), and the initial condition

$$\left[ 0.999, 0.99999, 0.997, 1.610 \times 10^{-2}, 4.980 \times 10^{-2}, 6.485 \times 10^{-4} \right]^T. \quad (32)$$

The evolution is shown in figure 6. Node 5 is the first to destabilize, followed by node 4. We also see that node 6 remains at its level because  $\epsilon$  is smaller than the threshold  $\epsilon_0$  for the static front of the type  $[1, 1, 1, 1, 1, 0]^T$ .

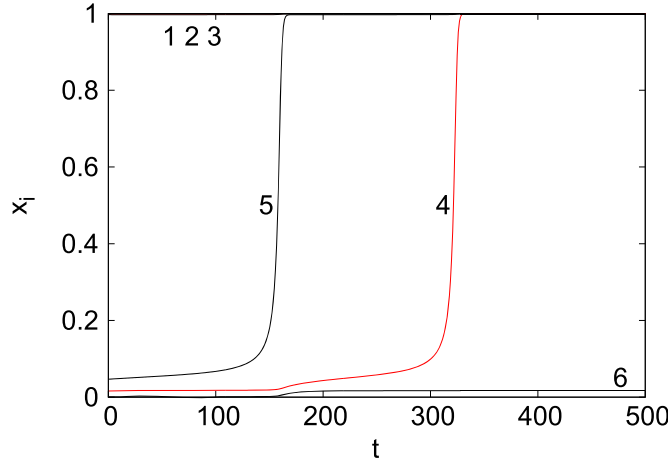


**Figure 6.** Time evolution of the different nodes for an initial front solution of the type  $[1, 1, 1, 0, 0, 0]^T$ , with  $\epsilon = 1.32 \times 10^{-3}$  and the initial condition (32).

One can estimate the time for  $x_5$  to grow, using the normal form displayed in figure 2 as a function of  $\delta = \epsilon - \epsilon_c$ . It gives

$$\dot{x}_5 = x_5^2 + \delta,$$

so that

$$x_5(t) = \sqrt{\delta} \tan(\sqrt{\delta}t), \tag{33}$$

which grows as  $1/\sqrt{\delta}$ . We have

$$\epsilon_c = 1.3 \times 10^{-3}, \quad \epsilon = 1.4 \times 10^{-3}, \quad \delta = 10^{-4}, \quad 1/\sqrt{\delta} = 100.$$

From figure 6 one sees that the typical time of destabilization of  $x_5$  is about 100 so the estimate is correct.

These results confirm that generalized static fronts exist for small  $\epsilon$  and disappear for  $\epsilon > \epsilon_c$ ; they are summarized in table 1. The above examples also suggest a qualitative picture of the propagation of fronts, where one can use the analytic expression (23) for  $\epsilon_0$  to guess the order in which the different nodes are excited. It appears that given a configuration of excited sites, the next site is the one in the neighborhood of the configuration that has the largest number of connections with the configuration connections. In the case where we have more than one such sites, the one that has the fewest connections, see e.g. the example of figure 3. This rule is consistent with the calculation of the smallest  $\epsilon_0$  values from (23) among the possible  $n_c$  in the vicinity of a configuration. This rule does not include all possibilities, but it points to a possible connection between the  $\epsilon_0$  for the various branches, and the propagation of the front. An estimation of  $\delta = \epsilon - \epsilon_0$  leads to an approximate time for the site  $n_c$  to be excited, using (33).

**5.2. Comparison between different solutions and front propagation models**

To illustrate the comparison of two initial conditions under the Zeldovich evolution, we show solutions from initial conditions  $[1, 1, 1, 0, 0, 0]^T$  and  $[1, 1, 0, 0, 0, 0]^T$  respectively. We

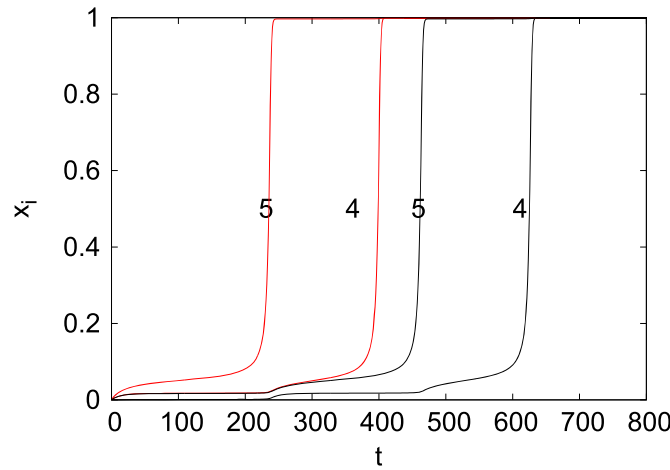


**Figure 7.** Time evolution of nodes 4 and 5 for the initial fronts  $[1, 1, 1, 0, 0, 0]^T$  in continuous line (red online) and  $[1, 1, 0, 0, 0, 0]^T$  in dashed line.

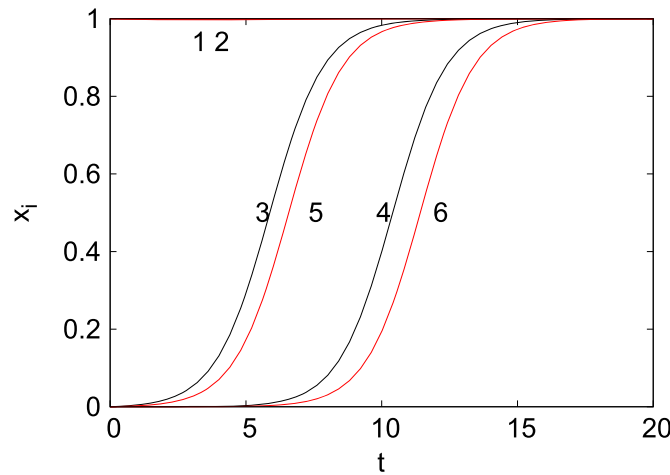


**Figure 8.** Time evolution of the initial front  $[1, 1, 0, 0, 0, 0]^T$ .

use  $\epsilon = 1.4 \times 10^{-3}$ . The time evolution is indicated figure 7 where the nodes 4 and 5 are shown. The trajectories increase faster for the first initial condition than for the second.

To illustrate the comparison between trajectories of the Fisher and Zeldovich equations we use the initial condition  $[1, 1, 0, 0, 0, 0]^T$ , with  $\epsilon = 1.4 \times 10^{-3}$ . It is presented in figure 8. Note that the scale in time is much shorter than in figure 7, here for  $t = 20$  the front has invaded the graph. Therefore the Fisher solution will always be larger than the Zeldovich one. Also the profile is different since there are no fixed points other than the flat 1 homogeneous state.

We also consider the evolution of the Kermack–McKendrick model (7). When the decay term  $\beta$  for the infected component  $i$  is zero, the evolution of  $i$  is identical to the one of the Fisher model (8). This is because (7) conserves  $s + i$ . For example taking as initial condition

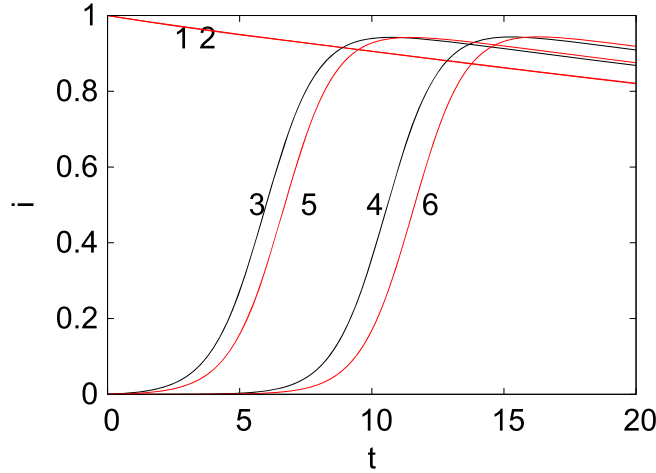


**Figure 9.** Time evolution of the infected component  $i$  for the initial front  $s = [0, 0, 1, 1, 1, 1]^T$ ,  $i = [1, 1, 0, 0, 0, 0]^T$  for the Kermack–McKendrick model (7) with  $\beta = 0.01$ .

$$s = [0, 0, 1, 1, 1, 1]^T, \quad i = [1, 1, 0, 0, 0, 0]^T$$

yields exactly the same dynamics for  $i$  as the one of figure 8. On the other hand, if we choose  $s + i < 1$  and still the same initial  $i$ , then the trajectories of (7) are below the ones of (8). Nevertheless the characteristic time for the orbits of (7) to reach saturation is the same as for (8). When  $\beta > 0$  is small, the infected component reaches a maximum in this characteristic time and then decays over a time scale  $1/\beta$  figure 9 shows the evolution of the infected component for  $\beta = 0.01$  and  $\epsilon = 1.35 \times 10^{-3}$ . To see propagation on the network,  $\beta$  should be smaller than the diffusion time  $1/\epsilon$ .

The comparisons between the Zeldovich models on the one hand, and the Fisher, and the Kermack–McKendrick models show that the latter two lead to a much faster propagation. This makes the comparison between the Fisher, and Kermack–McKendrick models a more interesting result.

The examples above suggest also that the order in which the different nodes become excited in the three models is the same. This order seems to depend only on the geometry of the graph. It may be possible to use different (possibly branch or site dependent) parameters  $\epsilon$ ,  $\gamma$ , and  $a$  for the Zeldovich and Fisher systems to make the propagation speeds comparable.

### 5.3. Influence of the parameter $a$

To conclude this numerical section, we consider how the fixed points of the Zeldovich equation and its dynamical solutions depend on the parameter  $a$ . To illustrate how  $a$  changes the fixed point and its subsequent destabilization, we consider the front centered on node 6 of the type  $[0, 0, 0, 0, 0, 1]^T$ . For  $a = 0.3$  and  $\epsilon = 1.25 \times 10^{-3}$  we obtain the static front

$$\left[ 0.104, 5.477 \times 10^{-2}, 0.107, 0.124, 0.295, 0.852 \right]^T. \tag{34}$$

Compared to the one for  $a = 0.1$  in (29), this front is much broader. Here we see that  $x_5 \approx a$  and  $x_3, x_4$  and  $x_1$  are close to  $a/2$ .

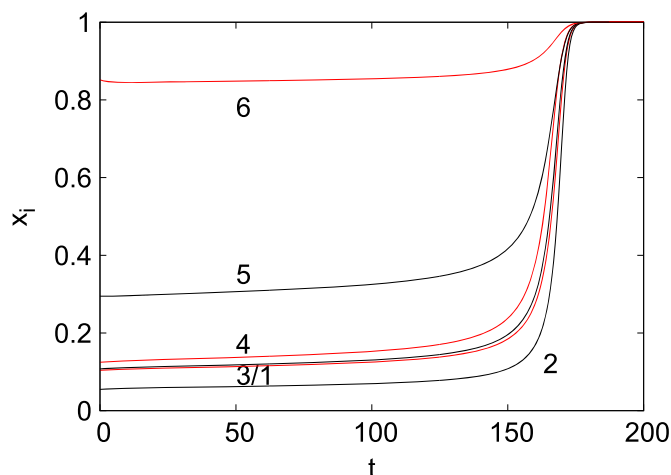


**Figure 10.** Time evolution for the initial condition  $[0.1036, 5.477 \times 10^{-2}, 0.107, 0.124, 0.294, 0.851]^T$  for  $\epsilon = 1.3 \times 10^{-1}$  close to the critical value  $\epsilon_0 = 1.25 \times 10^{-1}$  for the Zeldovich equation. The parameter  $a = 0.3$ .

**Table 2.** Critical  $\epsilon$  for the ‘generalized front’ centered on node 6 to destabilize for different values of  $a$ .

$a$	$\epsilon_0$	Expression (23)
0.1	$3.0 \times 10^{-3}$	$2.8 \times 10^{-3}$
0.2	$1.6 \times 10^{-2}$	$1.28 \times 10^{-2}$
0.3	$1.2 \times 10^{-1}$	$3.48 \times 10^{-2}$

The time evolution of the initial condition (34) is presented in figure 10. Note the large velocity with which the front ‘invades’ the network. For  $a = 0.1$ , in figure 3 we had a well separated dynamics of node 5 which destabilized first. Here we cannot distinguish the evolution of node 5 from the one of the other nodes. Since the front is much wider, it averages out the network and propagates much faster.

Because the front becomes very wide, the formula (23) will underestimate the critical  $\epsilon$ . Table 2 shows  $\epsilon_0$  for  $a = 0.1, 0.2$  and  $0.3$  obtained for the static solution centered on node 6. As expected (23) underestimates  $\epsilon_0$  as  $a$  increases. It gives the right order of magnitude for  $a = 0.2$  but is clearly wrong for  $a = 0.3$ .

## 6. Conclusion

We studied analytically and numerically a bistable reaction diffusion on an arbitrary finite network. We show that stable static fronts exist everywhere on the network for small diffusivity. We give the asymptotics of these fixed points and derive from them a simple depinning criterion which is validated both by continuation techniques and by solving the time dependent problem. The justification of the depinning criterion is an open problem, and may be related to the small value of the local excitation parameter  $a$ . The numerical simulations suggest that the moving front ‘feels’ the different static configurations, as it travels across the network.

We also compare different solutions of the Zeldovich model and show how ‘large’ fronts dominate ‘small’ fronts in the dynamics. A particularly interesting outcome of corollary (4.2), is that one can predict how complicated fronts will move by following simpler ones.

The time dependent solutions of the Fisher and Kermack–McKendrick original models are compared to the ones of the Zeldovich; they have a much shorter time scale and no threshold. This effect might be expected from the instability of the origin in the Fisher and Kermack–McKendrick models. This seems to reduce their interest as opposed to the Zeldovich model. On the other hand, all three models describe qualitatively similar front expansion scenarios above the Zeldovich threshold. The behavior of the Zeldovich model below the highest branch threshold may reflect some pinning phenomena related to epidemics. Finally we investigate numerically larger local excitation thresholds and show that fronts become wider and travel much faster across the network.

## Acknowledgments

JGC thanks the Universidad Nacional Autónoma de México for its hospitality during two visits. The work of JGC is supported partially by a grant from the Grand Réseau de Recherche, Transport Logistique et Information of the Haute-Normandie region. GC benefited from the support of UNAM grant PAPIIT-IN112713 and from a grant from the Fédération Normandie Mathématiques. PP acknowledges partial support from SEP-Conacyt grant 177246, and FENOMECC. The authors acknowledge the Centre de Ressources Informatiques de Haute Normandie for the computations together with Ana Perez and Ramiro Chavez from IIMAS-UNAM for technical support.

## Appendix A. Proof of propositions 3.3 and 3.1

The proof of proposition 3.3 uses the following intermediate result.

**Lemma A.1.** *Let  $x(0)$  be a nontrivial solution equation  $F = 0$  with  $\epsilon = 0$ , and let  $x(\epsilon)$ ,  $\epsilon \in [0, \epsilon_0]$  denote the unique branch of solutions of  $F = 0$ ,  $\epsilon > 0$ , that continue  $x(0)$  for  $\epsilon \geq 0$ . Consider the sets  $S_I$ ,  $S_a$ ,  $S_0$ , and  $I$  corresponding to  $x(0)$  as defined above, with  $S_I$ ,  $I$  nonempty. Then for  $\epsilon > 0$  sufficiently small we have that (i)  $n \in S_0$ ,  $\text{dist}(S_A, n) \geq m \geq 1$  imply*

$$x_n(\epsilon) = O(\epsilon^m), \quad (\text{A.1})$$

and (ii)  $n \in S_I$ ,  $\text{dist}(I, n) \geq m \geq 0$  imply

$$x_n(\epsilon) = 1 + O(\epsilon^{m+1}). \quad (\text{A.2})$$

**Proof.** We use the analytic version of the implicit value theorem, which allows us to write  $x_n(\epsilon)$  as a convergent power series in  $\epsilon$ , for  $\epsilon$  sufficiently near the origin. Thus we write  $x_n(\epsilon) = \sum_{m=0}^{\infty} a_{n,m} \epsilon^m$ , for all sites  $n$ , see e.g. [13]. (Since the network is finite it is sufficient to use the  $C^r$  version for  $r$  sufficiently large.)

We then already have  $x_n(\epsilon) = O(\epsilon)$ ,  $\forall n \in S_0$ , and  $x_n(\epsilon) = 1 + O(\epsilon)$ ,  $\forall n \in S_I$ .

To show (i) let  $n$  satisfy  $\text{dist}(S_A, n) \geq 2$ . We have

$$\begin{aligned} \epsilon(\Delta x)_n &= \epsilon \left[ -c_n \left( a_{n,1}\epsilon + O(\epsilon^2) \right) + \sum_{j \in \text{nbr}(n)} x_j \right] \\ &= O(\epsilon^2), \end{aligned} \tag{A.3}$$

since  $j \in \text{nbr}(n)$  implies  $j \in S_0$ , hence  $x_j = O(\epsilon)$ .

Also

$$x_n(1 - x_n)(a - x_n) = -aa_{n,1}\epsilon + O(\epsilon^2). \tag{A.4}$$

By (A.3), (A.4), and  $F = 0$  we must then have  $a_{n,1} = 0$ .

We use induction: suppose that if  $\text{dist}(S_A, n) \geq m \geq 2$ , then  $x_n = O(\epsilon^m)$ .

Then for  $n$  satisfying  $\text{dist}(S_A, n) \geq m + 1$  we have

$$\begin{aligned} \epsilon(\Delta x)_n &= \epsilon \left[ -c_n \left( a_{n,m}\epsilon^m + O(\epsilon^{m+1}) \right) + \sum_{j \in \text{nbr}(n)} x_j \right] \\ &= O(\epsilon^{m+1}), \end{aligned} \tag{A.5}$$

since  $j \in \text{nbr}(n)$  implies  $\text{dist}(S_A, j) \geq m$ , hence  $x_j = O(\epsilon^m)$  by the inductive hypothesis. On the other hand

$$x_n(1 - x_n)(a - x_n) = -aa_{n,m}\epsilon^m + O(\epsilon^{m+1}). \tag{A.6}$$

By (A.5), (A.6), and  $F = 0$  we must then have  $a_{n,m} = 0$ , and therefore  $x_n = O(\epsilon^{m+1})$ , as required.

To see (ii) let  $n \in S_1$  satisfy  $\text{dist}(I, n) = 1$ , so that all  $j \in \text{nbr}(n)$  satisfy  $x_j(0) = 1$ . Also  $x_n = 1 + O(\epsilon)$ . Then

$$\begin{aligned} \epsilon(\Delta x)_n &= \epsilon \left[ -c_n \left( 1 + a_{n,1}\epsilon + O(\epsilon^2) \right) + \sum_{j \in \text{nbr}(n)} x_j \right] \\ &= \epsilon \left[ -c_n - c_n a_{n,1}\epsilon + c_n + \sum_{j \in \text{nbr}(n)} a_{j,1}\epsilon + O(\epsilon^2) \right] \\ &= O(\epsilon^2). \end{aligned} \tag{A.7}$$

On the other hand

$$x_n(1 - x_n)(a - x_n) = -(a - 1)a_{n,1}\epsilon + O(\epsilon^2). \tag{A.8}$$

By (A.7), (A.8), and  $F = 0$  we must have  $a_{n,1} = 0$ , and therefore  $x_n = O(\epsilon^2)$ .

For the inductive step, assume that if  $n \in S_1$  satisfies  $\text{dist}(I, n) \geq m$ , then  $x_n = 1 + O(\epsilon^{m+1})$ . Consider then a site  $n$  satisfying  $\text{dist}(I, n) \geq m + 1$ , then

$$\begin{aligned}
 \epsilon(\Delta x)_n &= \epsilon \left[ -c_n \left( 1 + a_{n,m+1}\epsilon^{m+1} + O(\epsilon^{m+2}) \right) + \sum_{j \in \text{nbr}(n)} x_j \right] \\
 &= \epsilon \left[ -c_n - c_n a_{n,m+1}\epsilon^{m+1} + c_n + \sum_{j \in \text{nbr}(n)} a_{j,m}\epsilon^{m+1} + O(\epsilon^{m+2}) \right] \\
 &= O(\epsilon^{m+2}),
 \end{aligned} \tag{A.9}$$

using the fact that  $j \in \text{nbr}(n)$  implies  $\text{dist}(I, j) \geq m$ , hence  $x_j = 1 + O(\epsilon^{m+1})$  by the inductive hypothesis. On the other hand

$$x_n(1 - x_n)(a - x_n) = -(a - 1)a_{n,m+1}\epsilon^{m+1} + O(\epsilon^{m+2}). \tag{A.10}$$

By (A.9), (A.10),  $F = 0$  implies  $a_{n,m+1} = 0$ , and therefore  $x_n = 1 + O(\epsilon^{m+2})$ , as required.  $\square$

We now prove proposition 3.3.

**Proof.** The starting point is again the expression  $x_n(\epsilon) = \sum_{m=0}^{\infty} a_{n,m}\epsilon^m$ . To see (i) first consider sites  $n$  satisfying  $\text{dist}(S_A, n) = 1$ . Letting  $J_1$  be the set of sites  $j \in \text{nbr}(n) \cap S_A$ , and  $J_2 = \text{nbr}(n) \setminus J_1$ , we have

$$|J_1| = |\text{nbr}(n) \cap S_1| + |\text{nbr}(n) \cap S_a| > 0.$$

Then

$$\begin{aligned}
 \epsilon(\Delta x(\epsilon))_n &= \epsilon \left[ -c_n O(\epsilon) + \sum_{j \in J_1} x_j + \sum_{j \in J_2} x_j \right] \\
 &= (|\text{nbr}(n) \cap S_1| + |\text{nbr}(n) \cap S_a| a)\epsilon + O(\epsilon^2) \\
 &> 0
 \end{aligned} \tag{A.11}$$

for  $\epsilon > 0$  sufficiently small. On the other hand

$$x_n(1 - x_n)(x_n - a) = -a\epsilon a_{n,1} + O(\epsilon^2). \tag{A.12}$$

By (A.11), (A.12),  $F = 0$ , we need  $a_{n,1} > 0$ .

We proceed inductively, assuming that if  $n \in S_0$  satisfies  $\text{dist}(S_A, n) = m \geq 1$ , then  $x_n(\epsilon) = a_{n,m}\epsilon^m + O(\epsilon^{m+1})$ , with  $a_{n,m} > 0$ . Consider then a site  $n$  satisfying  $\text{dist}(S_A, n) = m + 1$ . Let  $J_m$  be the set of sites  $j \in \text{nbr}(n)$  satisfying  $\text{dist}(S_A, j) = m$ . Clearly  $|J_m| > 0$ . Also let  $J_{m+1} = \text{nbr}(n) \setminus J_m$ . By lemma A.1,  $x_n(\epsilon) = O(\epsilon^{m+1})$ . Then

$$\begin{aligned}
 \epsilon(\Delta x(\epsilon))_n &= \epsilon \left[ -c_n \left( a_{n,m+1}\epsilon^{m+1} + O(\epsilon^{m+2}) \right) + \sum_{j \in J_m} x_j + \sum_{j \in J_{m+1}} x_j \right] \\
 &= \sum_{j \in J_m} a_{j,m}\epsilon^{m+1} + O(\epsilon^{m+2}) \\
 &> 0
 \end{aligned} \tag{A.13}$$

for  $\epsilon > 0$  small, since  $a_{j,m} > 0, \forall j \in J_m$ , by the inductive hypothesis. On the other hand

$$x_n(1 - x_n)(x_n - a) = -a a_{n,m+1}\epsilon^{m+1} + O(\epsilon^{m+2}). \tag{A.14}$$

By (A.13), (A.14), and  $F = 0$ , we therefore need  $a_{n,m+1} > 0$ .

To see (ii) consider a site  $n \in S_1 \cap I$ , so that  $\text{dist}(I, n) = 0$ . Then  $x_n(\epsilon) = 1 + a_{n,1}\epsilon + O(\epsilon^2)$ , and

$$\begin{aligned} \epsilon(\Delta x(\epsilon))_n &= \epsilon[-c_n(1 + O(\epsilon)) + \sum_{j \in \text{nbr}(n) \cap S_1} x_j + \sum_{j \in \text{nbr}(n) \cap S_\alpha} x_j] \\ &= \epsilon(-c_n + |\text{nbr}(n) \cap S_1| + |\text{nbr}(n) \cap S_\alpha| a) + O(\epsilon^2). \end{aligned} \quad (\text{A.15})$$

Suppose  $\mu = |\text{nbr}(n) \cap S_\alpha| \geq 1$ , then  $|\text{nbr}(n) \cap S_1| \leq c_n - \mu$ , and (A.15) yield

$$\begin{aligned} \epsilon(\Delta x(\epsilon))_n &\leq \epsilon(-c_n + (c_n - \mu) + a\mu) + O(\epsilon^2) \\ &= (-1 + a)\mu\epsilon + O(\epsilon^2) \\ &< 0, \end{aligned} \quad (\text{A.16})$$

for  $\epsilon > 0$  sufficiently small. If  $\mu = 0$ ,  $n \in I$  implies  $|\text{nbr}(n) \cap S_1| < c_n$ , so that (A.15) implies

$$\begin{aligned} \epsilon(\Delta x(\epsilon))_n &\leq \epsilon(-c_n + (c_n - 1)) + O(\epsilon^2) \\ &= -\epsilon + O(\epsilon^2) \\ &< 0, \end{aligned} \quad (\text{A.17})$$

for  $\epsilon > 0$  sufficiently small. Combining (A.16) and (A.17) with

$$x_n(1 - x_n)(x_n - a) = -a_{n,1}(1 - a)\epsilon + O(\epsilon^2), \quad (\text{A.18})$$

we see that to satisfy  $F = 0$  with  $\epsilon > 0$ , sufficiently small we must have  $-a_{n,1} > 0$ .

For the inductive step, assume that  $n \in S_1$ ,  $\text{dist}(I, n) = m$  imply  $x_n(\epsilon) = 1 + a_{n,m+1}\epsilon^{m+1} + O(\epsilon^{m+2})$  with  $a_{n,m+1} < 0$ . Then let  $n \in S_1$ ,  $\text{dist}(I, n) = m + 1$ . Let  $J_m$  be the set of sites  $j \in \text{nbr}(n)$  satisfying  $\text{dist}(I, j) = m$ , let  $J_{m+1}$  be the set of sites  $j \in \text{nbr}(n)$  satisfying  $\text{dist}(I, j) \geq m + 1$ .

By lemma A.1 we have  $x_n(\epsilon) = 1 + O(\epsilon^{m+2})$ . Then

$$\begin{aligned} \epsilon(\Delta x(\epsilon))_n &= \epsilon \left[ -c_n(1 + O(\epsilon^{m+2})) + \sum_{j \in J_m} x_j + \sum_{j \in J_{m+1}} x_j \right] \\ &= \epsilon \left[ -c_n + |J_m| + \sum_{j \in J_m} a_{j,m+1}\epsilon^{m+1} + (c_n - |J_m|) + O(\epsilon^{m+2}) \right] \\ &= \sum_{j \in J_m} a_{j,m+1}\epsilon^{m+2} + O(\epsilon^{m+3}) \\ &< 0 \end{aligned} \quad (\text{A.19})$$

for  $\epsilon > 0$  sufficiently small, since  $a_{j,m+1} < 0, \forall j \in J_m$  by the inductive hypothesis. On the other hand

$$x_n(1 - x_n)(x_n - a) = -(1 - a)a_{n,m+2}\epsilon^{m+2} + O(\epsilon^{m+3}). \quad (\text{A.20})$$

By (A.19) and (A.20) to satisfy  $F = 0$  we must have  $-a_{n,m+2} > 0$ , as required.  $\square$

We now prove proposition 3.1.

**Proof.** To study large  $\epsilon$  solutions of  $F(x, \epsilon) = 0$  we will equivalently examine  $\mu \rightarrow 0^+$  solutions  $\tilde{F}(x, \mu) = 0$ , where

$$\tilde{F}_n(x, \mu) = (\Delta x)_n + \mu f_n(x), \tag{A.21}$$

$n = 1, \dots, N$ .

Then  $F(x, \epsilon) = 0, \epsilon > 0$ , is equivalent to  $\tilde{F}(x, \mu) = 0$ , with  $\mu = \epsilon^{-1}$ .

Consider a sequence  $\{(x_n, \epsilon_n)\}_{n \in \mathbf{Z}^+} \in I^N \times \mathbf{R}^+$ , satisfying  $\epsilon_n \rightarrow \infty$ , and  $F(x_n, \epsilon_n) = 0, \forall n \in \mathbf{Z}^+$ . Such sequences clearly exist. Moreover  $(x_n, \mu_n)$ , with  $\mu_n = (\epsilon_n)^{-1}$ , satisfy  $\tilde{F}(x_n, \mu_n) = 0, \forall n \in \mathbf{Z}^+$ . The sequence of solutions  $\{(x_n, \mu_n)\}_{n > n_0}$  of  $\tilde{F} = 0$  belongs to  $I^{N+1} = I^N \times [0, 1]$  for some  $n_0 > 0$ , and by the compactness of  $I^{N+1}$  has a convergent subsequence in  $I^{N+1}$ , denoted again as  $\{(x_n, \mu_n)\}_{n \in \mathbf{Z}^+}$ . Let  $(x_*, \mu_*)$  be the limit of this subsequence. By the assumption  $\epsilon_n \rightarrow \infty$ , we have that  $\mu_* = 0$ . Also,  $\tilde{F} : \mathbf{R}^{N+1} \rightarrow \mathbf{R}^{N+1}$  is continuous and therefore  $\tilde{F}(x_n, \mu_n) \rightarrow \tilde{F}(x_*, 0)$  as  $(x_n, \mu_n) \rightarrow (x_*, 0)$ . Therefore  $\tilde{F}(x_*, 0) = 0$ . Since  $\tilde{F}(x, 0) = \Delta x$  we have  $x_* \in V \cap I^N$ , where  $V = \{c[1, \dots, 1]^T \in \mathbf{R}^N : c \in \mathbf{R}\}$ , i.e. the kernel of  $\Delta$ .

We show that  $x_*$  can only be one of the  $c[1, \dots, 1]^T$ , with  $c = 0, a$ , or  $1$ . Let  $P$  the orthogonal projection of  $\mathbf{R}^N$  onto  $V$ . Also let  $W = I - P$ , where  $I$  the identity in  $\mathbf{R}^N$ . We apply  $P$  and  $I - P$  to  $\tilde{F} = 0$ , and write  $x = v + w$ , with  $v \in V, w \in W$ . This decomposition is unique. Using the facts that  $\Delta$  and  $P$  commute, and that  $\Delta v = 0, \tilde{F} = 0$  becomes

$$Pf(v + w) = 0, \tag{A.22}$$

$$\Delta w + \mu(I - P)f(v + w) = 0. \tag{A.23}$$

Fix any  $v \in V \cap I^N$ . We use the implicit function theorem to continue the solution  $(w, \mu) = (0, 0)$  of (A.23) to a solution with  $\mu \neq 0$ . Then for  $|\mu|$  sufficiently small there exists a one-parameter family of solutions  $(w, \mu) = (h(\mu; v), \mu)$  of (A.23), where  $h(\cdot; v)$  is continuous in  $\mu$ , with  $h(\mu; v) = O(\mu)$  as  $\mu \rightarrow 0$  (uniformly in  $v$ ). The implicit function theorem also implies that these solutions are the only solutions of (A.23) in a sufficiently small neighborhood of  $(w, \mu) = (0, 0)$  in  $W \times \mathbf{R}$ . Similar considerations show that the function  $h$  is continuous in  $v, \forall v \in v \in V \cap I^N$ .

Thus all solutions of  $\tilde{F}(x, \mu)$ , with  $x = v + w, v \in V, w \in W$ , and  $w \rightarrow 0, \mu \rightarrow 0$ , must be of the form  $x = v + h(\mu, v)$ , with  $v$  a solution of

$$g(v, \mu) = Pf(v + h(\mu; v)) = 0, \tag{A.24}$$

by (A.22).

Suppose that we have a sequence of solutions  $\{(v_n, \mu_n)\}_{n \in \mathbf{Z}^+}$  of  $g(v, \mu) = 0$  with  $v \in V \cap I^N$ , and  $\mu_n \rightarrow 0$ . By compactness this sequence has a convergent subsequence. Denote its limit by  $(v_*, 0)$ . By the continuity of  $h$ , and therefore of  $g, v_*$  must satisfy  $g(v_*, 0) = Pf(v_*) = 0$ , hence  $v_* = v_r = c_r[1, \dots, 1]^T, r = 1, 2, 3$  with  $c_1 = 0, c_2 = a, c_3 = 1$ . Applying the implicit function theorem again we check that each of the solutions  $v_r, r = 1, 2, 3$ , of  $g(v, 0) = 0$  is continued to a unique branch of solutions of  $g(v, \mu) = 0$ , with  $(v, \mu)$ . Each of these three branches contains all possible solutions of  $g = 0$  sufficiently near the respective  $(v_r, 0), r = 1, 2, 3$ . By uniqueness these three local branches are subsets of the three trivial branches  $(v_r, \mu), r = 1, 2, 3, \mu > 0$ , of solutions of  $\tilde{F} = 0$ .  $\square$

## Appendix B. Proof of comparison statements of section 4 (4.1, 4.3 and 4.4)

Consider a general ODE  $\dot{z} = F(z)$  in  $\mathbf{R}^K$  with initial condition  $z(0)$ , and the corresponding solution  $z$  in the interval  $[0, T]$ . Fix a positive integer  $M > 1$ , and let  $\Delta t = T/M$ . Let  $z^M$  be an array of  $M + 1$  vectors  $z^M(m\Delta t) \in \mathbf{R}^K$ ,  $m \in \{0, \dots, M\}$ , defined iteratively by  $z^M(0) = z(0)$ ,

$$z^M((m+1)\Delta t) = z^M(m\Delta t) + F(z^M(m\Delta t))\Delta t, \quad m \in 0, \dots, M. \quad (\text{B.1})$$

(The dependence of  $\Delta t$  on  $M$  is not explicit in this notation.) Thus  $z^M$  is the numerical trajectory obtained by the first order, explicit Euler method with constant time-step  $\Delta t = T/M$  over an interval  $[0, T]$ . We recall a standard convergence result for the Euler method (see e.g. [17]):

**Lemma B.1.** *Consider the ODE  $\dot{z} = F(z)$  in  $\mathbf{R}^K$  with initial condition  $z(0)$ , and assume that the solution  $z(t)$ ,  $t \in [0, T]$ , exists and is unique. Assume also that  $F$  is  $C^1$  in  $\mathbf{R}^K$ . For every integer  $M > 1$  let  $z^M$  be as in (B.1) with fixed time-step  $\Delta t = T/M$  over the interval  $[0, T]$ . Then*

$$\lim_{M \rightarrow \infty} \max_{m \in \{0, \dots, M\}} \|z(m\Delta t) - z^M(m\Delta t)\| = 0, \quad (\text{B.2})$$

where  $\|\cdot\|$  denotes the norm in  $\mathbf{R}^K$ .

In the following lemma we compare two Euler approximates of either the Zeldovich or the Fisher equations. We see that they preserve the order of the initial conditions.

**Lemma B.2.** *Let  $T > 0$ , and let  $M > 1$  be an integer. Let  $x^M, y^M$  be the Euler approximations with time-step  $\Delta t = T/M$  over the interval  $[0, T]$  of two trajectories of either the Zeldovich (9) or the Fisher (8) equations. Assume that  $x^M(0) < y^M(0)$ , with  $x^M(0), y^M(0)$  in  $[0, 1]^N$ . Then  $x^M(m\Delta t) < y^M(m\Delta t)$ ,  $\forall m \in \{1, \dots, M\}$ , provided  $M$  is sufficiently large.*

The lemma also implies that the Euler approximations of the Zeldovich and Fisher equations with initial conditions in  $[0, 1]^N$  stay in  $[0, 1]^N$ , provided the time-step is small enough.

The proof below shows that this step size does not depend on the initial conditions, it only depends on  $\Delta$ , i.e. the graph, and the functions

$$f_F(x) = (1-x)x, \quad f_Z(x) = (1-x)x(x-\alpha) \quad (\text{B.3})$$

in the equations.

**Proof.** Consider the first step of the iteration for the Zeldovich equation, starting with two initial conditions  $x^M(0) < y^M(0)$  in  $[0, 1]^N$ .

We have

$$\begin{aligned} y^M(\Delta t) - x^M(\Delta t) &= y^M(0) - x^M(0) \\ &+ \Delta t \left[ \epsilon \Delta (y^M(0) - x^M(0)) + f_Z(y^M(0)) - f_Z(x^M(0)) \right]. \end{aligned}$$

Examining the components of the  $y^M(\Delta t)$ ,  $x^M(\Delta t)$  we have that for every  $k \in \{1, \dots, N\}$ ,

$$y_k^M(\Delta t) - x_k^M(\Delta t) \geq \left[ 1 + \Delta t \left( -\epsilon n_k + f'_Z(\tilde{x}_k) \right) \right] \left( y_k^M(0) - x_k^M(0) \right), \quad (\text{B.4})$$

where  $\tilde{x}_k \in [0, 1]$ , and  $-n_k = \Delta_{k,k}$ .

To maintain the  $y_k^M(\Delta t) - x_k^M(\Delta t)$  positive it suffices that

$$1 + \Delta t \left( -\epsilon n_{\max} + \min_{x \in [0,1]} f'_Z(x) \right) > 0, \quad (\text{B.5})$$

with  $n_{\max} = \max_{k \in \{1, \dots, N\}} n_k$ . This can be achieved for  $M$  sufficiently large, and independent of  $y^M(0)$ ,  $x^M(0)$ .

Applying this argument to the case where either  $x^M(0) = \mathbf{0}$ , or  $y^M(0) = \mathbf{1}$ , both static solutions of the Zeldovich equation, we then have  $\mathbf{0} \leq x^M(\Delta t) < y^M(\Delta t) < \mathbf{1}$ , which also implies  $x^M(0), y^M(0) \in [0,1]^N$ . We can iterate the argument for all remaining steps, with the same step size  $T/M$ . The Fisher case is treated similarly.  $\square$

Similarly we compare Euler approximates of the Zeldovich and Fisher equations. We see that the Fisher approximations propagate faster. The proof also shows that  $(s(t), i(t))$  remains in  $\tau^N$  for all times.

**Lemma B.3.** *Let  $T > 0$ , and let  $M > 1$  be an integer. Let  $x_Z^M, x_F^M$  be the Euler approximations with time-step  $\Delta t = T/M$  over the interval  $[0, T]$  of the Zeldovich (9) and Fisher (8) equations respectively. Assume that  $x_Z^M(0) \leq x_F^M(0)$ , with  $x_Z^M(0), x_F^M(0)$  in  $[0,1]^N$ . Then  $x_Z^M(m\Delta t) < x_F^M(m\Delta t)$ ,  $\forall m \in \{1, \dots, M\}$ , provided  $M$  is sufficiently large.*

**Proof.** The argument is similar to the one used for lemma B.2 above and some details are omitted. Consider the first step of the iteration for the Zeldovich and Fisher equations, starting with respective initial conditions  $x_Z^M(0) < x_F^M(0)$  in  $[0,1]^N$ , and let  $f_Z, f_F$  denote the Zeldovich and Fisher nonlinearities respectively. We have

$$\begin{aligned} x_F^M(\Delta t) - x_Z^M(\Delta t) &= x_F^M(0) - x_Z^M(0) \\ &+ \Delta t \left[ \epsilon \Delta \left( x_F^M(0) - x_Z^M(0) \right) + f_F \left( x_F^M(0) \right) - f_Z \left( x_Z^M(0) \right) \right]. \end{aligned}$$

From

$$\begin{aligned} f_F \left( x_F^M(0) \right) - f_Z \left( x_Z^M(0) \right) &= \left[ f_F \left( x_F^M(0) \right) - f_F \left( x_Z^M(0) \right) \right] \\ &+ \left[ f_F \left( x_Z^M(0) \right) - f_Z \left( x_Z^M(0) \right) \right], \end{aligned} \quad (\text{B.6})$$

and

$$(1-x)x \geq (1-x)x(x-\alpha), \quad \alpha \in (0, 1), \forall x \in [0, 1],$$

the second expression in (B.6) is a positive vector. Collecting the analogues of the (B.4) for the components of  $x_F^M(\Delta t) - x_Z^M(\Delta t)$  we then have

$$x_F^M(\Delta t) - x_Z^M(\Delta t) \geq \left[ 1 + \Delta t \left( -\epsilon n_{\max} + \min_{x \in [0,1]} f'_F(x) \right) \right] \left( x_F^M(0) - x_Z^M(0) \right).$$

We can then take  $M$  sufficiently large and independent of the initial conditions so that  $\mathbf{0} \leq x_F^M(\Delta t) < x_Z^M(\Delta t) \leq \mathbf{1}$ , and repeat the argument for all steps.  $\square$

**Lemma B.4.** *Let  $T > 0$ , and let  $M > 1$  be an integer. Let  $x^M$ , and  $(s^M, i^M)$  be the Euler approximations with time-step  $\Delta t = T/M$  over the interval  $[0, T]$  of the Fisher (8) and Kermack–McKendrick (7) equations respectively. Assume that  $i^M(0) \leq x^M(0)$ , with  $x^M(0)$  in  $[0, 1]^N$ ,  $(s^M(0), i^M(0)) \in \tau^N$ . Then  $i^M(m\Delta t) < x^M(m\Delta t)$ ,  $\forall m \in \{1, \dots, M\}$ , provided  $M$  is sufficiently large. For such  $M$  we also have  $(s^M(m\Delta t), i^M(m\Delta t)) \in \tau^N$ ,  $\forall m \in \{1, \dots, M\}$ .*

**Proof.** The argument is similar to the one used for lemmas B.2, and some details are omitted. Consider the first step of the iteration for the Kermack–McKendrick and Fisher equations, starting with respective initial conditions  $x_F^M(0)$  in  $[0, 1]^N$ ,  $(s^M(0), i^M(0)) \in \tau^N$ . We have at each site  $k$

$$\begin{aligned} x_k^M(\Delta t) - i_k^M(\Delta t) &= x_k^M(0) - i_k^M(0) \\ &\quad + \Delta t \left[ \epsilon \left( \Delta \left( x^M(0) - i^M(0) \right) \right)_k \right. \\ &\quad \left. + x_k^M(0) \left( 1 - x_k^M(0) \right) - i_k(0) s_k(0) + \gamma i_k^M(0) \right]. \end{aligned} \quad (\text{B.7})$$

By  $s_n^M(0) + i_n^M(0) \leq 1$ , we therefore have

$$\begin{aligned} x_k^M(0) \left( 1 - x_k^M(0) \right) - i_k(0) s_k(0) &\geq x_k^M(0) \left( 1 - x_k^M(0) \right) - i_k(0) \left( 1 - i_k^M(0) \right) \\ &\quad + f'_F(\bar{x}_k) \left( x_k^M(0) - i_k^M(0) \right) \end{aligned} \quad (\text{B.8})$$

for  $\bar{x}_k$  in  $[i_k^M(0), x_k^M(0)] \subset [0, 1]$ . Then we have

$$i^M(\Delta t) - x^M(\Delta t) \geq \left[ 1 + \Delta t \left( -\epsilon n_{\max} + \min_{x \in [0, 1]} f'_F(x) \right) \right] \left( x^M(0) - i^M(0) \right), \quad (\text{B.9})$$

and therefore  $i^M(\Delta t) < x^M(\Delta t)$  for  $M$  sufficiently large and independent of the initial conditions.

A similar argument is used to show that  $s^M(\Delta t), i^M(\Delta t) > 0$  for  $M$  sufficiently large and independent of the initial conditions, and we omit the details.

By lemma B.2 similarly have  $x^M(\Delta t) \in [0, 1]^N$  for  $M$  sufficiently large and independent of the initial conditions. Finally adding the Euler formulas for  $s^M(\Delta t), i^M(\Delta t)$ , and using  $\Delta \mathbf{1} = 0$ , we have

$$\begin{aligned} \mathbf{1} - \left( s^M(\Delta t) + i^M(\Delta t) \right) &= \mathbf{1} - \left( s^M(0) + i^M(0) \right) \\ &\quad + \Delta t \left[ \epsilon \left( \mathbf{1} - \left( s^M(0) + i^M(0) \right) + \gamma i^M(0) \right) \right] \\ &\geq \left( 1 - \Delta t \epsilon d_{\max} \right) \left[ \mathbf{1} - \left( s^M(0) + i^M(0) \right) \right], \end{aligned} \quad (\text{B.10})$$

which is positive for  $M$  sufficiently large and independent of the initial conditions. We can then iterate the argument for the remaining steps.  $\square$

The fact that the convergence of the approximate solutions  $x^M$  of the Euler method to the trajectory  $x$  in lemma B.2 preserves the partial order follows from the following.

Let  $\{g^M\} = \{g_M\}_{M=1}^\infty$ , denote a sequence of arrays (of increasing size  $M + 1$ )  $g^M = (g_0^M, \dots, g_M^M)$  of vectors  $g_m^M \in \mathbf{R}^K$ ,  $m = 0, \dots, M$ . Let  $\{g^M\} \rightarrow g$  denote that

$$\lim_{M \rightarrow \infty} \max_{m \in \{0, \dots, M\}} \|g_m^M - g(m(T/M))\| = 0, \quad (\text{B.11})$$

where  $g: [0, T] \rightarrow \mathbf{R}^K$ , and  $\|\cdot\|$  is the norm in  $\mathbf{R}^K$ .

**Lemma B.5.** Consider sequences  $\{g^M\}$ ,  $\{h^M\}$  as above satisfying that for all  $M$  sufficiently large we have that  $g_m^M < h_m^M$ ,  $\forall m \in \{0, \dots, M\}$ . Suppose also that there exist continuous functions  $g, h: [0, T] \rightarrow \mathbf{R}^K$  for which  $\{g^M\} \rightarrow g$ , and  $\{h^M\} \rightarrow h$  respectively. Then  $g(t) \leq h(t)$ ,  $\forall t \in [0, T]$ .

**Proof.** The statement follows from continuity of  $h - g$  in  $[0, T]$ , since it is easy to see that  $h(t_0) - g(t_0) > 0$  for some  $t_0 \in (0, T]$  and the convergence leads to a contradiction.  $\square$

We now prove proposition 4.1.

**Proof.** Combining the comparison of approximate solutions produced by the Euler method lemma B.2, with the approximation lemmas B.1, B.5 we have that  $x(0) < y(0)$  implies  $x(t) \leq y(t)$ ,  $\forall t \in [0, T]$ . To show the strict inequality we use the fact that the evolution can be also defined uniquely also backwards in time. Thus  $x(t) \leq y(t)$ , for some  $t \in (0, T]$  leads to a contradiction.  $\square$

Propositions 4.3 and 4.4 follow in the same way, but we can not apply the backwards evolution argument, and do not have strict inequality.

## References

- [1] Scott A C 2003 *Nonlinear Science, Emergence and Dynamics of Coherent Structures* (Oxford: Oxford University Press)
- [2] Nabarro F R N 1947 Dislocations in a simple cubic lattice *Proc. R. Soc.* **59** 256–72
- [3] Keener J P 1987 Propagation and its failure in coupled systems of discrete excitable cells *SIAM J. Appl. Math.* **47** 556–72
- [4] Erneux T and Nicolis G 1993 Propagating fronts in discrete bistable reaction–diffusion system *Physica D* **67** 237–44
- [5] Carpio A and Bonilla L 2003 Depinning transitions in discrete reaction–diffusion equations *SIAM J. Appl. Math.* **63** 1056–82
- [6] Hoffman A and Mallet-Paret J 2010 Universality of crystallographic pinning *J. Dyn. Diff. Eqns.* **22** 79–119
- [7] Cvetkovic D, Rowlinson P and Simic S 2001 *An Introduction to the Theory of Graph Spectra* (London Mathematical Society Student Texts vol 75 (Cambridge: Cambridge University Press)
- [8] Cruz-Pacheco G, Duran L, Esteva L, Minzoni A A, Lopez-Cervantes M, Panayotaros P, Ahued-Ortega A and Villaseñor Ruiz I 2009 Modelling of the influenza A(H1N1) outbreak in Mexico City, April–May 2009, with control measures *Eurosurveillance* **14** 19254
- [9] MacKay R S and Aubry S 1994 Proof of existence of breathers for time-reversible or Hamiltonian networks of weakly coupled oscillators *Nonlinearity* **7** 1623–43
- [10] Kermack W O and McKendrick A G 1927 A contribution to the mathematical theory of epidemics *Proc. R. Soc. A* **115** 700–21
- [11] Murray J D 2003 *Mathematical Biology* vol 2 (Berlin: Springer)
- [12] Caputo J-G, Knippel A and Simo E 2013 Oscillations of networks: the role of soft nodes *J. Phys. A: Math. Theor.* **46** 035101
- [13] Zeidler E 1986 *Nonlinear Functional Analysis and its Applications I* (New York: Springer)
- [14] Powell M J D 1970 A hybrid method for nonlinear equations *Numerical Methods for Nonlinear Algebraic Equations* ed P Rabinowitz (New York: Gordon and Breach)
- [15] Keller H B 1977 Numerical solution of bifurcation and nonlinear eigenvalue problems *Applications of Bifurcation Theory* ed P H Rabinowitz (New York: Academic)
- [16] Hairer E, Norsett S P and Wanner G 1987 *Solving Ordinary Differential Equations I* (Berlin: Springer)
- [17] Iserles A 2008 *First Course in the Numerical Analysis of Differential Equations* 2nd edn (Cambridge: Cambridge University Press)